Depolarized-light-scattering study of orthoterphenyl and comparison with the mode-coupling model

W. Steffen, A. Patkowski,* H. Gläser, G. Meier, and E. W. Fischer
Max-Planck-Institut für Polymerforschung, Ackermannweg 10, 55128 Mainz, Germany
(Received 26 July 1993)

The dynamics of the molecular glass-forming liquid orthoterphenyl above the glass-transition temperature was studied combining several experimental techniques: depolarized Raman, depolarized Rayleigh-Brillouin light scattering, and photon correlation spectroscopy in the temperature range from 250 to 440 K. The combined spectra covering a frequency range from 10^{-2} to 10^{13} Hz were analyzed using the mode-coupling theory. The coordinates of the susceptibility minimum, $\omega_{\min}$ and $\chi_{\min}$, as well as the position of the maximum, $\omega_{\max}$ (α peak), scale with temperature according to the mode-coupling theory, resulting in $T_c = 290$ K. The construction of the predicted master curve in the vicinity of the minimum of the rescaled susceptibility was possible in a narrow frequency range only if the values of $\omega_{\min}$ resulting from the mode-coupling-theory force fit were used. The width of the α peak appears to increase with increasing temperatures for temperatures above T_c, although when the effects of fast processes on the high-frequency wing are included, the corrected width appears to decrease instead approaching a Debye relaxation shape at high temperatures. Below T_c it was not possible to fit objectively the data using the mode-coupling theory; thus it was impossible to corroborate the divergence of the scaling time of the mode-coupling β relaxation on both sides of T_c. Assuming *a priori* that the mode-coupling model is correct, it is possible to make the data compatible with the mode-coupling theory.

PACS number(s): 61.25.Em, 33.20.Fb, 64.70.Pf

INTRODUCTION

The dynamics of the van der Waals glass-forming liquid orthoterphenyl (OTP) has been described in terms of separated dynamic processes ([1], and references cited therein). The primary (α) relaxation has been characterized in a broad temperature range above the glass-transition temperature by means of dielectric spectroscopy [2], dynamic light scattering (DLS) [1], NMR [3], and quasielastic neutron scattering (QENS) [4]. The temperature dependence of the α relaxation time is Arrhenius-like at high temperatures and can be described by the Williams-Landel-Ferry (WLF) or Vogel-Fulcher-Tamann (VFT) formulas at low temperatures [1]. Another β_{JG} process (Johari and Goldstein [2]) with an Arrhenius temperature dependence was found in OTP in a dielectric-spectroscopy study. Additionally, a fast process analyzed as a single Lorentzian of practically constant relaxation time of the order of 1 ps and intensity decreasing to zero at the ideal glass transition (VFT) temperature T_0 was found in a DLS study on OTP [1]. A similar process was reported in neutron scattering experiments for OTP [5,4] and tri-α-naphtylbenzene (TNB) [6]. All these processes are common features of low-molecular-weight and polymeric glass-forming liquids. In some of them additional processes were observed which could be related to the intramolecular relaxation [7]. This phenomenological description of the dynamics of glass-forming liquids in terms of separated processes does not result from any complete theory.

An alternative approach was adopted in the mode-coupling theory (MCT), where some characteristic features of a spectrum covering a broad frequency range (several orders of magnitude) are discussed [8,9]. The MCT predicts a β relaxation which cannot be identified with the β_{JG} process mentioned above since it occurs at much higher frequencies and has a different temperature dependence as reported in DLS [10,11] and QENS [5,4] experiments. Experimental spectra which can be analyzed using the MCT can be obtained in a DLS experiment using a combination of a Raman spectrum and spectra from a tandem Fabry-Pérot interferometer (T-FPI) of different free spectral ranges [10,11]. In this paper we have extended the frequency range of the data by additionally using a confocal FPI (C-FPI) and photon correlation spectroscopy (PCS). This extension is very important because it allows one to measure the α peak and the minimum of the susceptibility at temperatures below T_c.

The predictions of the idealized MCT have been tested previously using DLS [10,11] and QENS [5,4] data. It has been shown that the experimental data are compatible with the MCT in terms of predicted specific features of the susceptibility spectrum.

In this paper we present a critical test of the predictions of the idealized MCT using DLS spectra of OTP covering the frequency range from 10^{-2} to 10^{13} Hz. We discuss extensively the difficulties one encounters using the MCT to fit the experimental data: (i) the master-curve construction in the vicinity of the susceptibility minimum for $T > T_c$, (ii) temperature dependence of the width of the α peak, and (iii) difficulties in obtaining an objective estimate of the scaling time of the MCT β relaxation below T_c and its divergence at T_c.

*Also at the Institute of Physics, A. Mickiewicz University, Poznan, Poland.

THEORY

The mode-coupling theory and its application to analyze the dynamic-light-scattering data of glass-forming liquids have been extensively discussed elsewhere [8,9,12]. Here we will repeat only those predictions of the idealized MCT which can be tested using our experimental data.

β RELAXATION

The MCT predicts that the susceptibility $\chi''(\omega)$ can be expressed in terms of the scaling function $\chi''_{\pm}(\omega/\omega_\sigma)$ in the form

$$\chi''(\omega)=h_q|\sigma|^{1/2}\chi''_{\pm}\left[\frac{\omega}{\omega_\sigma}\right], \tag{1}$$

where σ is the separation parameter which in the vicinity of T_c is defined as

$$\sigma=C\frac{T_c-T}{T_c}. \tag{2}$$

ω_σ is the scaling frequency, h_q is a critical amplitude, and $\pm$ refers to $\sigma>0$ or $\sigma<0$, respectively, and C is a proportionality constant of the order of unity. For $T>T_c$ in the vicinity of the minimum the susceptibility can be approximated by an interpolation formula:

$$\chi''(\omega)=\frac{\chi''_{\min}}{a+b}\left[b\left[\frac{\omega}{\omega_{\min}}\right]^a+a\left[\frac{\omega}{\omega_{\min}}\right]^{-b}\right], \tag{3}$$

where $\omega_{\min}$ and $\chi''_{\min}$ are the frequency and the amplitude of the susceptibility minimum. The exponents a, b, and γ and the exponent parameter λ fulfill the following relations:

$$0<a\le 0.395,\quad 0<b\le 1, \tag{4}$$

$$\gamma=\frac{1}{2a}+\frac{1}{2b}, \tag{5}$$

$$\lambda=\frac{\Gamma^2(1-a)}{\Gamma(1-2a)}=\frac{\Gamma^2(1+b)}{\Gamma(1+2b)}. \tag{6}$$

The MCT predicts the following scaling of the parameters $\chi''_{\min}$ and $\omega_{\min}$ with temperature close to T_c:

$$\chi''_{\min}\propto\chi''_\sigma\propto|\sigma|^{1/2}, \tag{7}$$

$$\omega_{\min}\propto\omega_\sigma\propto|\sigma|^{1/2a}. \tag{8}$$

For $T<T_c$ the MCT predicts a change at ω_σ from a linear frequency dependence much below ω_σ: $\chi''(\omega)=\chi''_\sigma(\omega/\omega_\sigma)$ to a critical frequency dependence much above ω_σ: $\chi''(\omega)=\chi''_\sigma(\omega/\omega_\sigma)^a$. In this case χ''_σ and ω_σ refer to the amplitude and position of a "knee" in a plot of $\log_{10}[\chi''(\omega)]$ versus $\log_{10}(\omega)$.

The susceptibility spectrum corresponding to the β relaxation can be numerically calculated [13] as shown in Fig. 1, where $\log_{10}[\chi''(\omega)/\chi''_\sigma]$ is plotted versus $\log_{10}(\omega/\omega_\sigma)$. The upper master curve corresponds to $\sigma<0$ ($T>T_c$) and the lower one to $\sigma>0$ ($T<T_c$). In this representation both master curves have a limiting slope of a for $\omega\gg\omega_\sigma$. At frequencies $\omega\ll\omega_\sigma$ the slope amounts to $-b$ (von Schweidler exponent) for $T>T_c$ and to 1 for $T>T_c$.

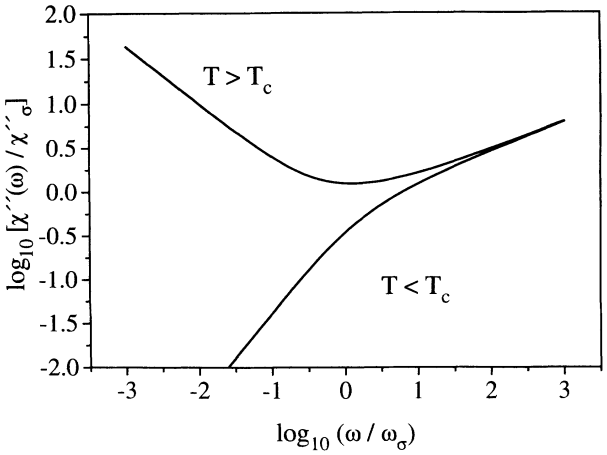

FIG. 1. The MCT master functions for temperatures above and below T_c. The curves were calculated using a $\lambda=0.70$ from the expansion coefficients given in Ref. [13].

α PROCESS

The idealized MCT predicts the α process to occur only for $T>T_c$ and to be completely frozen below T_c. The correlation function describing the α process in MCT is found to have a temperature-independent form thus obeying the time-temperature superposition principle. It has also been shown that the Kohlrausch-Williams-Watts (KWW) (stretched exponential) function

$$\Phi(t)=A\exp\left\{-\left[\frac{t}{\tau_{\rm KWW}}\right]^\beta\right\} \tag{9}$$

is a good approximation of the MCT correlation function, except at short times. Thus the MCT predicts a constant KWW β parameter above T_c. The susceptibility in the α region depends only on the scaling frequency ω'_σ:

$$\chi''(\omega)=\hat{\chi}''(\omega/\omega'_\sigma). \tag{10}$$

The position of the maximum of the susceptibility should obey the scaling law

$$\omega_{\max}\propto\omega'_\sigma\propto|\sigma|^\gamma. \tag{11}$$

EXPERIMENT

Orthoterphenyl of 97.5% purity was obtained from Merck-Schuchardt. This OTP was recrystallized several times from methanol solutions. Finally the sample was vacuum distilled into dust-free light-scattering cells (round, 10 mm inner diameter), which were flame sealed afterwards. High purity and a good optical quality of the samples resulted in a low Landau-Placzek ratio $R_{\rm LP}$ of 0.3 at 423 K. These samples were kept at room temperature for several months without a trace of crystallization.

The purified OTP has a glass transition temperature T_g of 244 K determined by differential scanning calorimetry (heating and cooling rates 5, 10, and 20 K/min) and a melting temperature of 329 K [differential scanning calorimetry (DSC)] in a good agreement with previously reported values [14].

Previously it was found that OTP can be prepared in two metastable states, with and without long-range density fluctuations [15]. The samples with long-range density fluctuations show a strong excess isotropic Rayleigh component leading to R_{LP} 20 to 50 times higher than expected for a viscoelastic liquid. In a previous depolarized-dynamic-light-scattering study no influence of the long-range density fluctuations on the relaxation times of the optical anisotropy fluctuations was found [1]. Therefore we performed our experiments on samples without long-range density fluctuations, to prevent any distortion of the spectra due to a leakage of the polarized light resulting from imperfections of polarizers, cryostat windows, etc.

All measurements reported here were done in *VH* geometry (polarizer and analyzer in crossed positions) to obtain the depolarized component of the light-scattering spectrum under a scattering angle $\Theta=90°$. We have combined measurements using a six-pass tandem Fabry-Pérot interferometer [T-FPI, Sandercock, free spectral ranges (FSR): 10, 15, 20, 50, 150, 450 GHz], and a confocal Fabry-Pérot interferometer (C-FPI, Burleigh CFT 100, FSR 750 MHz) with measurements done with a double-grating monochromator (SPEX 1403, 1800 lines/mm, focus 850 mm), and with a digital correlator (ALV5000 with fast option) for photon correlation spectroscopy (PCS). The C-FPI with a free spectral range of 750 MHz was used to measure the depolarized Rayleigh-Brillouin (DRB) spectra in the frequency range from 10 to 400 MHz.

Previously the DRB spectra of Salol and $CaKNO_3$ (CKN) [10,11] were measured in the frequency range from 0.2 GHz to 3.5 THz in the backscattering geometry. The extension of the experimental frequency window down to 10 MHz is very important and necessary in order to be able to measure the minimum in the susceptibility spectrum at temperatures close to and below T_c.

Our measurements were performed at a scattering angle $\Theta=90°$ using a modified experimental system in which no additional static light was necessary to stabilize the T-FPI. In this way undistorted DLS spectra, including the central peak, were measured at all temperatures. This central peak is mainly due to the first-order scattering resulting from optical anisotropy of the scattering medium. Its width is decreasing with decreasing temperatures and at low temperatures it is buried in the instrumental line while the integrated intensity is practically constant [1]. In the previous studies [10,11] most of the intensity within the instrumental line was due to the (elastic) light reflected from the surface of the cell, which was necessary to stabilize the T-FPI. Thus the central part of the spectrum could not be measured.

Figure 2 shows a schematic representation of the light-scattering experiment using tandem Fabry-Pérot interferometer. A single-mode argon-ion laser (Spectra Physics, model 2020), $\lambda=514.5$ nm with a typical power of 200 mW at the sample, was used as a monochromatic light source. The measurements with the C-FPI were performed using the second harmonic of a cw Nd-YAG (where YAG denotes yttrium aluminum garnet) laser (ADLAS, model 425) at a wavelength of 532 nm. This laser has a line which is narrower (<1 MHz) and more stable in frequency compared to the argon-ion laser. Again a typical power of 200 mW at the sample was achieved. The same Nd-YAG laser was used for the PCS measurements.

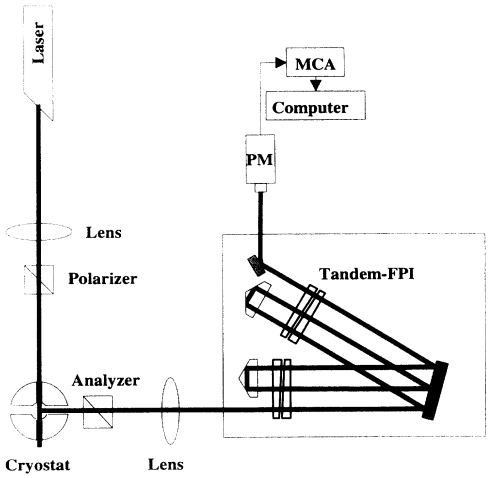

FIG. 2. Schematic representation of the experimental setup of the light-scattering experiment using the Tandem Fabry-Pérot interferometer (T-FPI).

In the Raman experiment a krypton-ion laser (Spectra Physics), $\lambda=647$ nm, and a typical power of 200 mW at the sample was used. The difference in the scattering vector $|\mathbf{q}|=q=(4\pi n/\lambda)\sin(\Theta/2)$ (n is the index of refraction, λ is the wavelength of incident light) due to the different wavelengths used in the experiments, is not expected to have an influence on the general structure of the scattering curves in *VH* geometry. This was shown for the case of Salol [10] and CKN [11], where no dependence on q was found. Only the transverse phonons display a strong q dependence of their spectral features, but they are not being looked at in the following MCT analysis. Glan prisms (Halle, Berlin) with an extinction coefficient better than 10^{-6} and Glan-Thompson prisms (Halle) with extinction coefficient better than 10^{-7} were used as polarizers and analyzers, respectively. The temperature of the sample was maintained by means of a cryostat (Oxford, model CF1204) in the case of the Raman and PCS experiment and by a specially constructed cryostat in the case of the FPI measurements. The sample temperature was kept constant to within ± 0.1 K using an Oxford ITC4 temperature controller and was measured with calibrated thermocouples mounted close to the sample.

A schematic diagram of the FPI experiment is depicted in Fig. 2. The incident light is focused by a lens into the scattering volume inside of the sample. A Glan prism between the lens and the cryostat selects only the vertical component of the incident light. The horizontally polar-

ized scattered light (*VH* component) at a scattering angle Θ, in our case always 90°, is selected by means of a Glan Thompson polarizer. A lens leads the divergent scattered light as a parallel bundle onto the FPI plates. After passing through the FPI the light is detected by a photomultiplier (PM, Thorn EMI, model 9893b/100-S) and the spectrum is accumulated in a multichannel analyzer (MCA). For further analysis the spectra are transferred to a computer.

Each section of the experimental DRB spectrum consisted of 600 points. In the combined spectrum the total number of points amounted to about 1000 due to the matching procedures. To match the overlap regions of the spectra of different FSR it was necessary to multiply the intensity at a given temperature with a constant. All spectra were matched to those of a FSR of 50 GHz. The spectra at this FSR were taken with great care for reproducibility. Since the external noise and the dark count of the photomultipliers used play no role in our spectra, an additive constant had not to be used in the matching procedure, leading to a greater reliability of the form of the compound spectra. The Stokes and anti-Stokes sides of the spectra agreed in intensity within the experimental error. Since in the following analysis only the positive frequencies are used, an average over the two sides was taken.

The spectra from the C-FPI were first corrected for the instrumental function. Up to four Lorentzians as central lines were convoluted with the instrumental function to describe the spectrum in as model independent a way as possible. A higher number of Lorentzians were found not to change the result. In this procedure two neighboring orders were taken into account on each side of the spectrum to remove overlap effects. This superposition of lines was then used in the matching procedure.

The experimentally available frequency range can be additionally extended by combining the DRB spectra with spectra covering a frequency range of 10^{-2} to 10^{6} Hz obtained by transforming the depolarized correlation functions measured by means of photon correlation spectroscopy. A direct Fourier transform of the measured correlation functions did not result in satisfactory spectra, because the cutoff effects caused a substantial distortion of the high-frequency part of the spectrum. This high-frequency tail is, however, necessary to match these spectra to the measured DRB spectra. We have found that another procedure of transforming the correlation functions results in much better spectra: (i) a correlation function covering a broad time range from 50 ns to 100 s is fitted with CONTIN [16] in order to obtain a distribution function of relaxation rates, and (ii) this distribution function was then used to simulate a spectrum in a corresponding frequency range. This transformation procedure was tested on simulated data with different noise levels. The transformations time-frequency-time resulted in final correlation functions practically identical to the initial ones. This procedure was used at low temperatures $T_g < T < T_c$ where the α process is out of the experimental frequency range of the FPI but can be easily measured by means of PCS and where the measurements with the C-FPI provided the minimum in the susceptibility spectrum. The slope on the high-frequency side of the PCS spectra matched the slope of the C-FPI spectra on their low-frequency side of the minimum within experimental error. A vertical shift introducing an amplitude factor for the PCS spectra was sufficient to match the spectra. Nevertheless over about one order of magnitude an extrapolation of the PCS spectra was necessary to bridge the gap between FPI and PCS range.

RESULTS AND DISCUSSION

The composite DRB spectra measured in the temperature range from 250 to 440 K are shown in Fig. 3. From the DRB spectra $I(\omega)$ (Fig. 3), the susceptibility spectra $\chi''(\omega)$ (Fig. 4) were calculated as

$$\chi''(\omega)=\frac{I(\omega)}{[n(\omega)+1]} , \tag{12}$$

where the Bose factor can be expressed as

$$n(\omega)+1 \propto \frac{kT}{\hbar\omega} . \tag{13}$$

The intensity and susceptibility spectra obtained for OTP in this work are qualitatively similar to the corresponding spectra measured previously for Salol [10], however, a broader frequency range was covered in our experiment and we performed the measurement at a scattering angle of 90° instead of in a backscattering geometry as in [10] (no q dependence for these spectra is expected).

As shown in Fig. 3, the DRB spectra, besides the expected relaxation processes, contain two additional features: (i) a transverse phonon peak at a few GHz with intensity decreasing with decreasing temperature, and (ii) a broad boson peak at about 400 GHz. The transverse

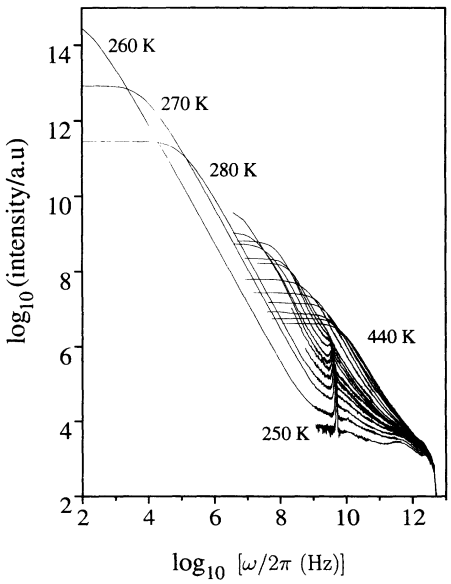

FIG. 3. Combined depolarized-light-scattering spectra in a double logarithmic plot. From bottom to top the temperatures are 250, 260, 270, 280, 285, 290, 295, 300, 305, 310, 315, 320, 340, 360, 380, 400, 420, and 440 K.

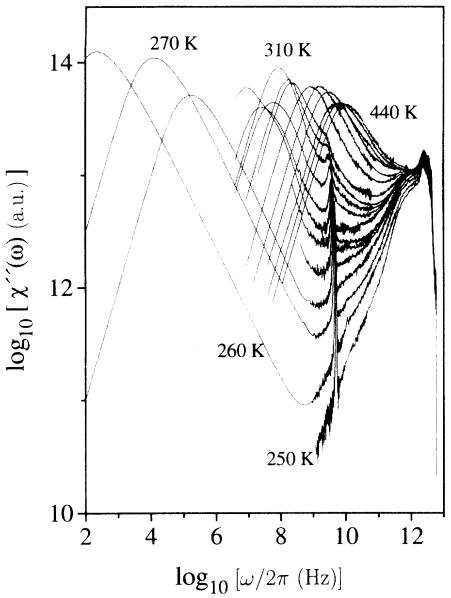

FIG. 4. Susceptibility $\chi''(\omega)$ of OTP obtained from the spectra in Fig. 3 using Eq. (12).

phonon peak can be easily removed from the spectra since it distorts only a narrow frequency range. The boson peak, however, is very broad and its position and intensity depend on temperature [17]. So it is not possible to remove it by simple subtraction of low-temperature data as is usually done in the QENS experiments. The properties of the transverse phonon and the boson peaks will be discussed in a separate paper [17]. For this reason all the DRB spectra in this work were analyzed only up to about 400 GHz, in a similar way as was done for Salol [10].

The DRB spectra (Fig. 3) and corresponding susceptibility spectra (Fig. 4) exhibit some of the features predicted by the MCT: At the highest temperatures the main α peak extends almost to the microscopic frequency in the THz range. With decreasing temperature the α peak is shifted to lower frequencies and a distinct minimum appears in the susceptibility spectra. With temperature approaching T_c the position of the minimum is shifted to lower frequencies.

At T_c the α peak and the minimum do not disappear, as predicted by the idealized version of the MCT. This is explained in the extended MCT by the additional contribution of the so-called activated hopping processes [12]. At temperatures below T_c the susceptibility spectra still show the α peak and the minimum which eventually move out of the frequency window of the FPI experiment and can be measured by means of PCS. The boson peak is increasing in intensity and shifting to higher frequencies with decreasing temperature in our temperature window above T_g, while the positions of peaks at even higher frequencies (i.e., optical modes) remain practically unchanged.

The most counterintuitive prediction of the MCT is a decrease of the scaling frequency of the β relaxation with increasing temperature below T_c (corresponding to a τ_β^+ getting longer). A "knee" (the scaling frequency) should appear in the susceptibility curves, marking the transition from a slope of one to a slope with the value of a. The position of this knee should move with temperature in the manner described above. Although in some of the data measured below T_c a "knee"-like shape appears, it does not have all the features predicted by the MCT. This, in part, may be due to the fact that part of the frequency range where the knee should appear is substantially distorted by the boson peak whose contribution is increasing with decreasing temperature. Similar problems were reported previously for Salol [10].

TESTING THE SCALING LAWS OF THE MCT

β relaxation

For temperatures above T_c the MCT predicts that in the vicinity of the minimum the susceptibility spectrum can be expressed by Eq. (3) with the constraints given by Eqs. (4)–(6). In our analysis the position $\omega_{\min}$ and the amplitude $\chi''_{\min}$ at the minimum were obtained in the following ways.

(i) The susceptibility spectra were fitted with a polynomial in the temperature range from 290 to 380 K (Fig. 5).

$$[\chi''(\omega)]=(\chi''_{\min})+A[\log_{10}(\omega)-\log_{10}(\omega_{\min})]^2 +B[\log_{10}(\omega)-\log_{10}(\omega_{\min})]^4 +C[\log_{10}(\omega)-\log_{10}(\omega_{\min})]^6 . \quad (14)$$

The rescaled susceptibility plot of $\chi''(\omega)/\chi''_{\min}$ versus $\omega/\omega_{\min}$ using the values of $\chi''_{\min}$ and $\omega_{\min}$ obtained from the polynomial fit is shown in Fig. 6.

(ii) Each susceptibility spectrum was independently fitted with Eq. (3). These two fits resulted in practically identical values of $\omega_{\min}$ and $\chi''_{\min}$ for each spectrum. The exponents a and b are changing with temperature (Table I), i.e., the data cannot be described by a master curve as predicted by the idealized MCT. Above T_c the suscepti-

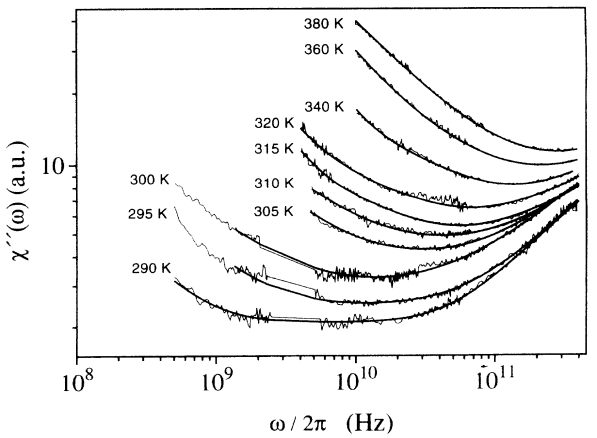

FIG. 5. Fit to the minimum in the susceptibilities above T_c using a polynomial [Eq. (14)].

TABLE I. Resulting fit parameters for the polynomial, MCT free fit, and MCT forced fit to the minimum region in $\chi''(\omega)$.

	Polynomial fit		Free MCT fit with interpolation formula				MCT fit, $\lambda=0.70$ $a=0.33; b=0.65$	
T (K)	χ''_{min} (a.u.)	ω_{min} (GHz)	χ''_{min} (a.u.)	ω_{min} (GHz)	a	b	χ''_{min} (a.u.)	ω_{min} (GHz)
290	2.10	6.71	2.00	6.74	0.68	0.21	1.83	5.34
295	2.53	12.04	2.42	14.16	0.58	0.37	2.37	9.54
300	3.26	13.93	3.23	14.62	0.49	0.45	3.21	11.56
305	4.29	30.69	4.28	31.63	0.55	0.41	4.45	23.73
310	4.91	42.13	4.88	40.18	0.43	0.57	5.00	35.66
315	5.42	56.22	5.41	53.11	0.42	0.56	5.54	49.92
320	6.48	68.31	6.64	61.16	0.33	0.62	6.74	64.34
340	8.23	135.32	8.31	132.60	0.40	0.56	8.32	124.60
360	9.93	214.94	9.98	214.30	0.26	0.74	9.86	253.80
380	11.33	281.04	11.37	237.50	0.53	0.60	11.30	344.10

bility spectra are getting steeper with increasing temperature.

We note that the scaling behavior predicted by idealized MCT should produce temperature-independent values of a and b. However, in the extended MCT, since the trajectory followed in the (σ,δ) parameter plane crosses successive scaling curves as T is lowered, scaling only holds approximately [12].

Finally, Eq. (3) was fitted to all the data with identical values of the exponents a and b for all temperatures between 290 and 380 K. The values of a and b were fixed at $a=0.33, b=0.65$, which results in $\lambda=0.70$ obtained from a free fit at high temperature (320 K). The fit is also reasonable (Fig. 7), however, as one can see in Table I, the positions ω_{min} obtained from this MCT forced fit are different from those obtained from the free fit, i.e., the values of ω_{min} are shifted to lower frequencies. This difference is increasing with decreasing temperature. Using the values of χ''_{min}, ω_{min} obtained from the MCT forced fit with fixed a and b one can construct a master plot which is reasonably well described by a master curve in a limited frequency range (Fig. 8).

The temperature dependence of ω_{min} and χ''_{min} obtained from the MCT forced fit is shown in Fig. 9. According to the predictions of the MCT $(\omega_{min})^{2a}$ and $(\chi''_{min})^2$ are linear functions of temperature. The extrapolated values of the temperature T_c are 287 K (from ω_{min}) and 292 K (from χ''_{min}) and are identical within experimental error. This value of T_c is in good agreement with a previously reported value of 290 K obtained from the quasielastic neutron scattering experiment [4].

Below T_c the MCT predicts that the slope of the susceptibility in a double logarithmic plot should change from 1 to a in the vicinity of ω_σ (see Fig. 1). To see how far one can describe those low-temperature data with a common master function we have computed the derivatives of the spectra and of the master function (see Fig. 1) for $\lambda=0.70$. To get rid of the influence of noise in the spectra we first parametrized the spectra with a polynomial, which was describing the finer details of the spectra (knees).

As one can see in Fig. 10, none of the derivatives, even for a small frequency range, is identical in shape with the

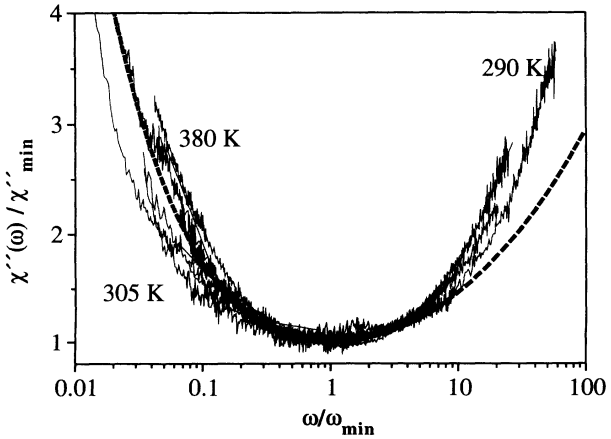

FIG. 6. Rescaled susceptibility plots of $\chi''(\omega)/\chi''_{min}$ vs ω/ω_{min} using ω_{min} and χ''_{min} obtained from the polynomial fit. The broken line is a master curve corresponding to $\lambda=0.70$.

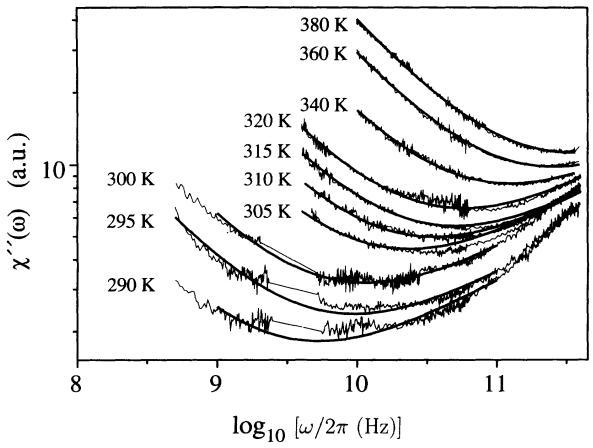

FIG. 7. Fit to the minimum in the susceptibilities above T_c using the interpolation formula [Eq. (3)] and fixed $a=0.33$ and $b=0.65$ parameters (fulfilling the λ constrain, $\lambda=0.70$) obtained from a fit to $T=320$ K data.

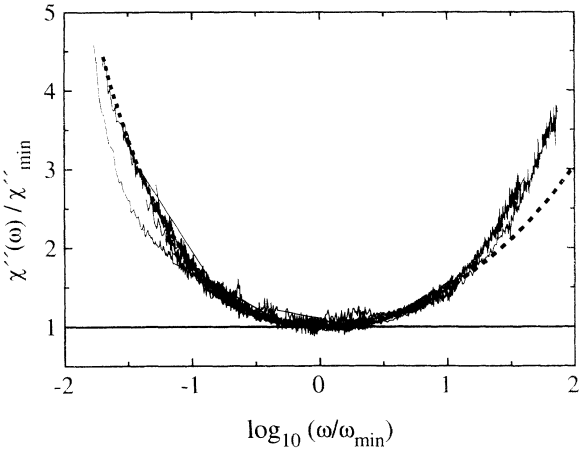

FIG. 8. Rescaled susceptibility plots of $\chi''(\omega)/\chi''_{\min}$ vs $\omega/\omega_{\min}$ using $\omega_{\min}$ and $\chi''_{\min}$ obtained from the forced fit with the interpolation formula (Fig. 5). The dashed line is a master curve corresponding to $\lambda=0.70$.

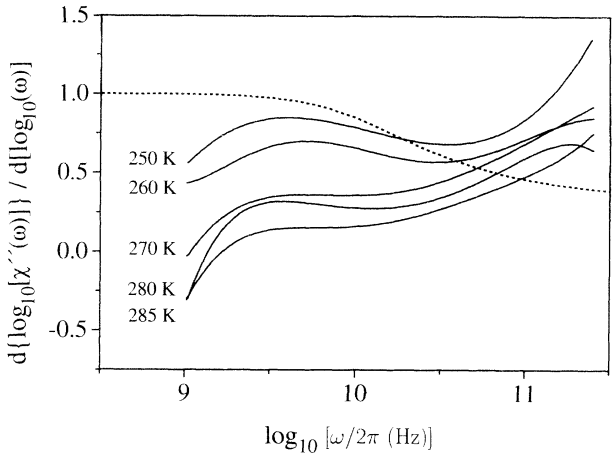

FIG. 10. Derivatives of the logarithm of the susceptibility with respect to the logarithm of the frequency. The broken line is this derivative of the master function below T_c.

derivative of the master function, thus no fit of the master function to the data is possible at $T < T_c$.

A closer look at the susceptibility in this frequency range reveals a "knee"-like structure at temperatures of 250 and 260 K resembling the master function. In Fig. 11 a master function at those two temperatures was fitted to the data in a narrow frequency range. With this procedure as much overlap as possible between master function and spectra was obtained. At higher temperatures of 270, 280, and 285 K no "knee" can be seen.

At low frequencies the spectra lie above the master function. This behavior might be explained by the presence of a minimum between the α relaxation or the hopping process discussed in the extended MCT, and the boson peak/microscopic excitations. At high frequencies the master curve deviates from the data close to the appearance of the boson peak which is not included in the MCT.

The temperature dependence of the values of ω_σ and χ''_σ obtained in this way is shown in Figs. 12(a) and 12(b). As one can see, the $\tau_\beta^+ = 1/\omega_\sigma$ is diverging at T_c in qualitative agreement with the MCT prediction [Eq. (8)] (results, however, in a different $T_c \cong 278$ K) while χ''_σ is changing at random in contradiction to Eq. (7).

The absolute values of $\tau_\beta^+ = 1/\omega_\sigma$ are much larger than the corresponding values of $\tau_\beta^- = 1/\omega_{\min}$ above T_c at the same distance from T_c so Eq. (8) is not fulfilled.

In order to obtain $\tau_\beta^\pm$ symmetrically diverging on both sides of T_c as reported previously [10,11] one would have to shift the corresponding master curves to much higher frequencies, Figs. 13, 14. The fit is much worse than the one in Fig. 11 and it was obtained in the following way: (i) τ_β^+ values were generated as a mirror reflection of τ_β^- values symmetrically to the axis $T = T_c = 290$ K, Fig. 14(a). (ii) The master curves were shifted horizontally

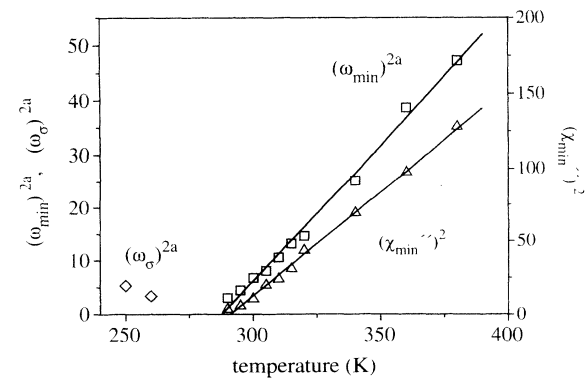

FIG. 9. Temperature dependence of $(\omega_{\min})^{2a}$ and $(\chi''_{\min})^2$ for $T > T_c$. The linear fits result in $T_c = 287$ K and $T_c = 292$ K, respectively. For the low temperatures ($T < T_c$) a fit to $(\omega_\sigma)^{2a}$ leads to a T_c of 278 K.

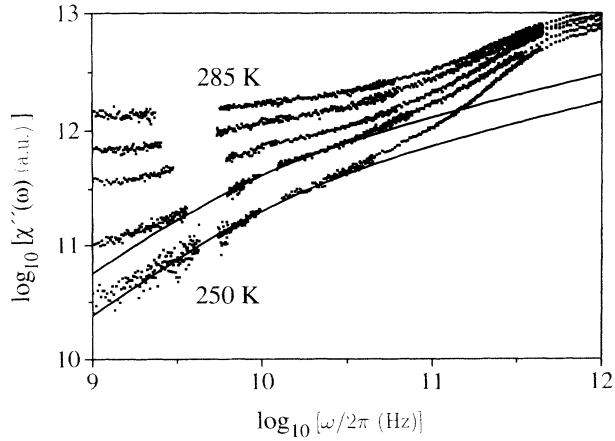

FIG. 11. Susceptibility at 250, 260, 270, 280, and 285 K in a limited frequency range. The solid lines represent the MCT master functions.

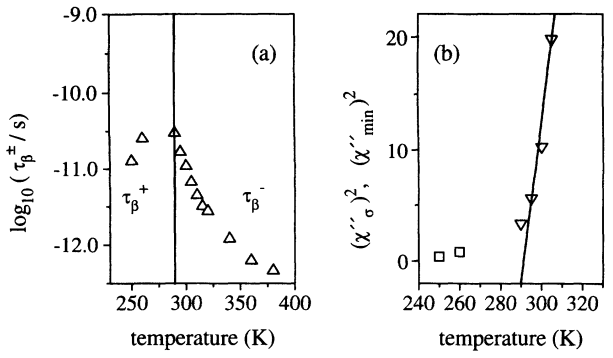

FIG. 12. (a) Plot of $\log_{10}(\tau_\beta^+)$ ($\triangle$) and (b) $(\chi''_\sigma)^2$ ($\square$) vs temperature for the master curves of Fig. 11. The values above T_c of τ_β^- ($\triangle$) in (a) and $(\chi''_{min})^2$ (∇) in (b) are taken from Fig. 9. τ_β^+ is much longer than τ_β^- measured at the same distance from T_c. χ''_σ does not scale as predicted by the MCT.

and the "knee" was positioned at the frequency $\omega_\sigma = 1/\tau_\beta^+$ (Fig. 13). The master curves were shifted vertically in order to obtain an overlap region between the data and the master curves. In this way the values of χ''_σ were obtained, which fulfill the predictions of the MCT [Eq. (7)] quite well, Fig. 14(b). Comparing these two fits (Figs. 11, 13) one can see that the fit in Fig. 11 is much better, however, the scaling behavior of τ_β^+ and χ''_σ is much worse (Fig. 12) than for the corresponding values of the forced fit shown in Fig. 14. Thus one can conclude that in the case of OTP it is not possible to fit the master curve to the data at $T < T_c$ using any reasonable objective criteria. It is, however, possible to perform a biased analysis by forced fitting of the predictions of the MCT.

This biased analysis is possible due to the generally observed feature of the data, i.e., that the slope of $\log_{10}[\chi''(\omega)]$ versus $\log_{10}(\omega)$ is decreasing with increasing temperature in the frequency range between the minimum and the microscopic frequency.

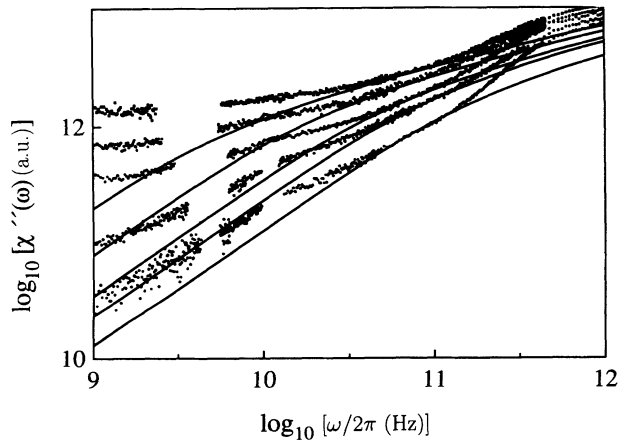

FIG. 13. Another fit of the master curves to the experimental data for $T < T_c$.

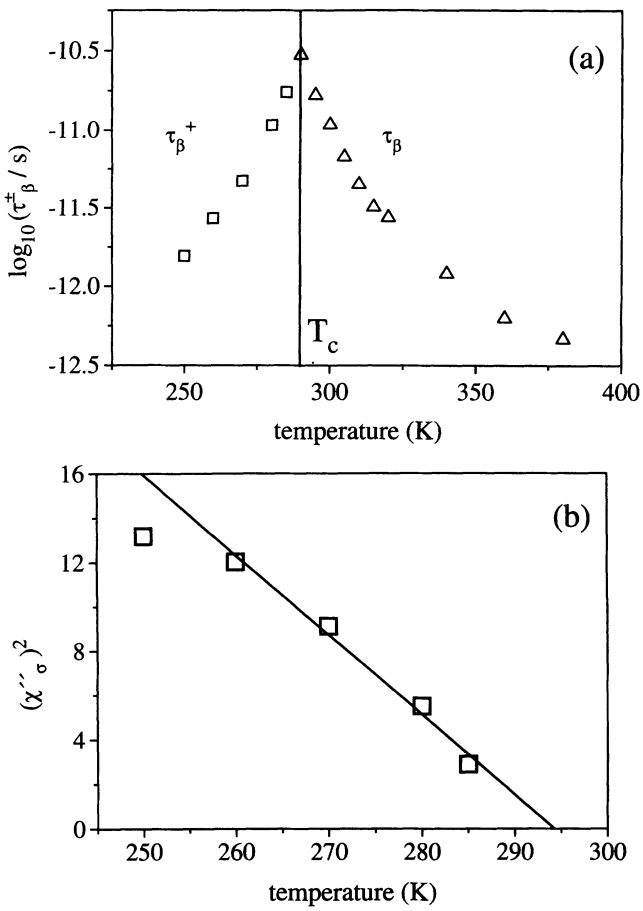

FIG. 14. Plot of generated τ_β^+ and experimental τ_β^- values (a), and corresponding χ''^-_σ values (b) obtained from the fit of Fig. 13 ($T < T_c$) and from Fig. 9 ($T > T_c$).

The α process

High-temperature susceptibility spectra in which the α process appears as a well-developed peak are shown in Fig. 15. The $\chi''(\omega)$ spectra, in the frequency range corresponding to the α process, have a slope of 1 for $\omega < \omega_{max}$ and are getting broader with increasing temperature for $\omega > \omega_{max}$. Based on a previous analysis of OTP spectra [1] we could attribute this unusual behavior to the fact that with increasing temperature the α peak is approaching the fast process at about 30 GHz [1] which has a constant position and intensity proportional to $(T - T_0)^2$, where T_0 is the (Vogel) ideal glass transition temperature. Alternatively, using the MCT picture, the α peak is approaching the MCT β relaxation which occurs even closer to the α peak and its intensity is also increasing with increasing temperature.

Thus with increasing temperature above T_c the fit of the α peak becomes ambiguous because of the overlap of the α and β relaxations on the high-frequency side of the peak. A direct fit of the KWW function to the entire peak results in apparent β_{KWW} which is decreasing with increasing temperature. If we fit the spectrum, in an al-

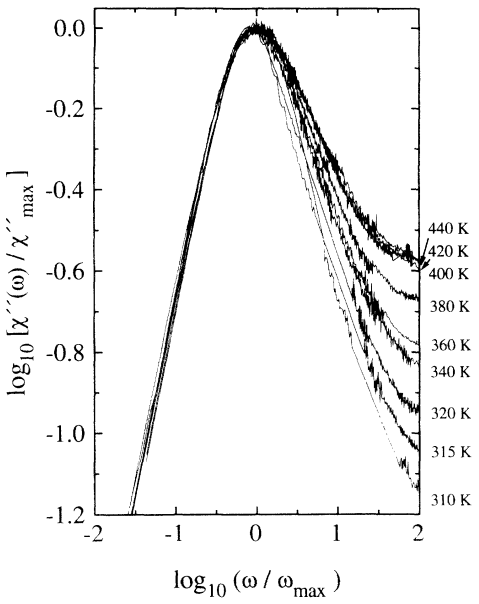

FIG. 15. Rescaled susceptibilities in the region of the α peak.

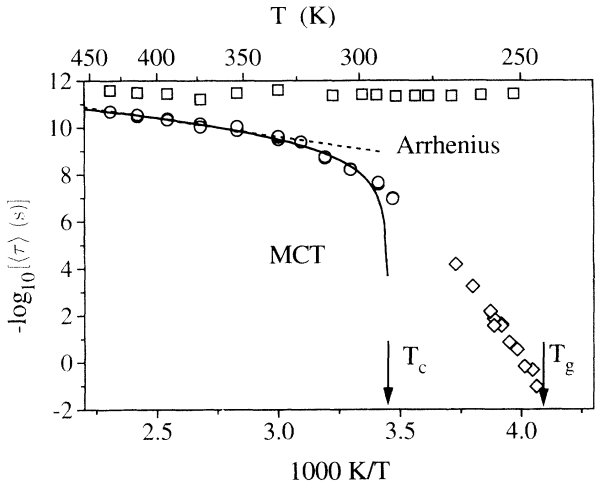

FIG. 17. Activation plot of OTP: □, fast process from [1]; ○, α process obtained from FPI experiment [1]; and ◇, α process obtained from PCS experiment [1]. The lines represent a MCT (solid) and an Arrhenius (broken) fit to the high-temperature data.

ternative approach, as a sum of the α process (KWW) and a fast process (Lorentzian) [1] we obtain the β_{KWW} increasing to about 1 with increasing temperature (Fig. 16), in agreement with the configurational-space percolation theory [18]. The β_{KWW} at temperatures below 275 K were obtained from a direct fit to the KWW function to the depolarized correlation function measured by means of PCS.

Above T_c the temperature dependence of the position of the maximum of the α peak which corresponds to the relaxation time of the α process τ_α can be equally well described by the MCT, Eq. (10) and an Arrhenius dependence, Fig. 17. Only in a narrow temperature range close to T_c does the MCT formula better describe the data. The MCT predicts that $(\omega_{max})^{1/\gamma}$ should be a linear function of temperature, Eq. (10). In Fig. 18 $(\omega_{max})^{1/\gamma}$ and $(\omega_{min})^{2a}$ are plotted versus temperature using the parameters obtained from the MCT forced fit to the susceptibilities: $a=0.33, b=0.65$, and $\gamma=2.25$. Both quantities exhibit a linear temperature dependence and extrapolate to zero at the same temperature $T_c=288$ K as predicted by the MCT.

According to the predictions of the MCT $\log_{10}(\chi''_{min})$ and $\log_{10}(\omega_{min})$ should be linear functions of $\log_{10}(\omega_{max})$ with slopes of $1/(2\gamma)$ and $1/(2a\gamma)$, respectively. This linear dependence is fulfilled reasonably well, Fig. 19. The obtained slopes amount to 0.238 [predicted: $1/(2\gamma)=0.222$] and 0.699 [predicted: $1/(2a\gamma)=0.673$], in good agreement with theoretically predicted values.

According to Eqs. (7) and (8) $\log_{10}(\chi''_{min})$ should be a linear function of $\log_{10}(\omega_{min})$ with a slope of a. Such a plot is shown in Fig. 20. The dependence is linear but the slope amounts to 0.495 and is much higher than the predicted one: $a=0.33$. Similar disagreement with this pre-

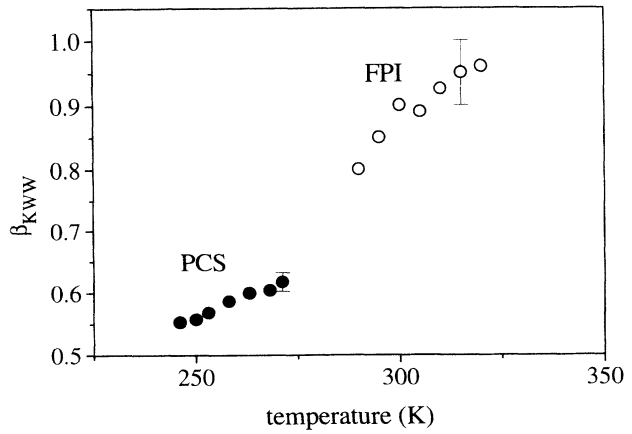

FIG. 16. Temperature dependence of the β_{KWW} parameter of the KWW function fitted to the α relaxation in the PCS and FPI data.

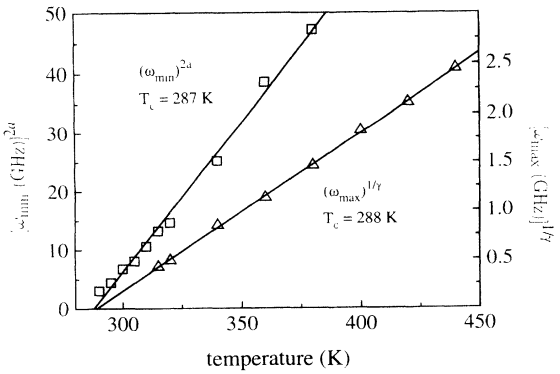

FIG. 18. Temperature dependence of $(\omega_{min})^{2a}$ and $(\omega_{max})^{1/\gamma}$. The values are obtained from the MCT forced fit to the data.

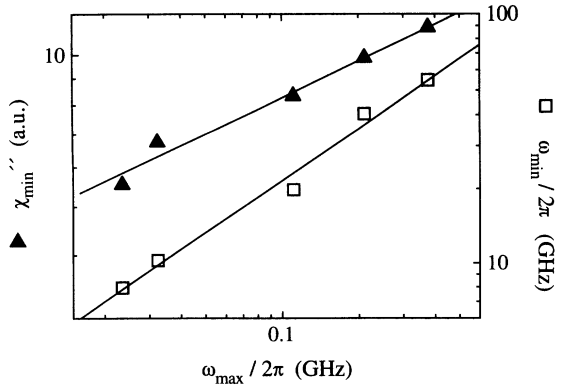

FIG. 19. Double logarithmic plot of χ''_{min} and ω_{min} vs ω_{max}.

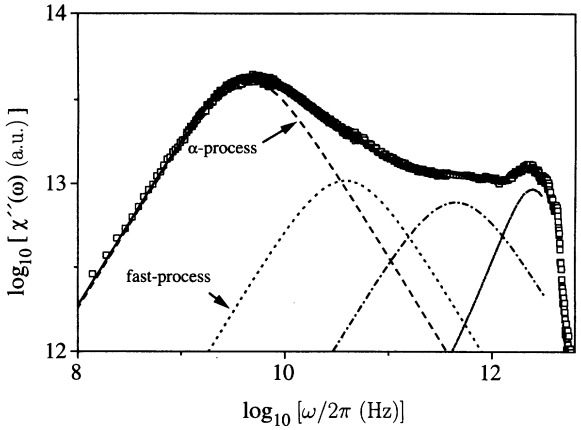

FIG. 21. Susceptibility $\chi''(\omega)$ of OTP at 400 K fitted with a superposition of Lorentzians for the α (— — —) and fast process (---) and two further Lorentzians (—·—·— and ——— ———) to take care of the contribution of microscopic excitations at high frequencies.

diction of the idealized MCT was also observed for Salol [10] and CKN [11] but was explained in an "extended MCT" analysis [12].

In order to check how unique the features of the susceptibility predicted by the MCT are, we have, alternatively, fitted our experimental data with a phenomenological model: α peak (KWW function with temperature-dependent width) + fast process (Lorentzian) + boson peak + microscopic excitations at even higher frequencies than the boson peak [19].

In Fig. 21 such a fit to the susceptibility measured at 400 K is shown. As one can see, the entire susceptibility covering more than four decades in frequency is fitted very well with this model. Such a procedure was used previously [1] by us to fit DRB spectra of OTP in the temperature range from T_g to T_g+200 K. The fast process obtained in this way has intensity decreasing to zero at T_0 and a practically temperature-independent relaxation time of about 1 ps in contrast to the scaling time of the MCT β relaxation which diverges on both sides of T_c.

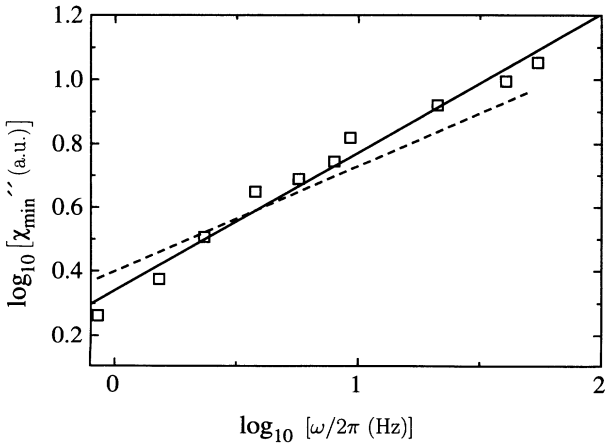

FIG. 20. Double logarithmic plot of χ''_{min} vs ω_{min}. The solid lines represent a linear regression to the data and the dashed line corresponds to the expected slope of $a=0.33$.

CONCLUSIONS

We have applied the idealized mode-coupling theory to analyze the susceptibility spectra of OTP covering 11 decades in frequency measured by a combination of depolarized-light-scattering techniques.

The MCT predicts that a plot of rescaled susceptibilities, $\chi''(\omega)/\chi''_{min}$ versus ω/ω_{min} at all temperatures above T_c in the β region, should result in a master curve with two adjacent power laws. In practice such a master curve can be obtained in a narrow frequency range around the minimum only if the values of ω_{min} and χ''_{min} are obtained from a forced fit using the interpolation formula [Eq. (3)] and fixed values of the exponents a and b. The coordinates of the minimum obtained from this forced fit do not describe the real minimum of the susceptibility. A free fit of the interpolation formula to the data results in temperature-dependent values of exponents a and b in contrast to the MCT. No master-curve construction is possible if the experimental values of ω_{min} and χ''_{min} are used. However, the scaling predictions of the MCT concerning temperature dependence of ω_{min} and χ''_{min} are well fulfilled, resulting in $T_c=290$ K in a very good agreement with previous QENS studies [5].

The temperature dependence of the position of the susceptibility maximum ω_{max} which corresponds to the α process is as predicted by the MCT at temperatures $T>T_c+20$ K. However, an Arrhenius fit is equally good in most of the temperature range except about 20–30 K above T_c. After taking the influence of the fast process on the high-frequency wing of the α process into account, the width of the α peak is decreasing with increasing temperature. The α peak and the minimum do not disappear at T_c in contrast to the predictions of the idealized MCT, consistent with the requirement that activated hopping terms must be included to provide a reasonable description of the low-frequency spectra below T_c.

Below T_c the MCT predicts that, in the β-relaxation region, the slope of the double logarithmic plot of the susceptibility should change from 1 (at low frequencies) to the value of the exponent a (at high frequencies) resulting in a "knee" at a frequency $\omega_\sigma = 1/\tau_\beta^+$. The most counterintuitive prediction of the MCT is that the scaling time τ_β^+ should increase with temperatures increasing towards T_c. We show that in the case of OTP (which is similar to Salol [10]) there is no unambiguous way to fit the master curve to the data in this frequency range. Therefore it is not possible to obtain unique (unbiased) values of the scaling time τ_β^+. The data can, however, be made compatible with the MCT using a biased fit, which results in the coordinates of the "knee" scaling with temperature according to the predictions to the MCT.

Previously a substantial improvement of the quality of the fit for CKN and Salol was achieved using the extended version of the MCT [12]. Such an analysis of our OTP data is currently underway.

Despite the problems discussed above several open questions remain concerning the mode-coupling analysis of depolarized-light-scattering data: (i) is the MCT fully applicable to the DLS results, (ii) what is the physical nature of the MCT β relaxation, (iii) is the scaling time of the β relaxation really diverging on both sides of T_c or is it constant as indicated by our previous experiments [1] and a recent simulation [20], (iv) what transition occurs at the temperature T_c and what is its relation to the calorimetric glass transition at T_g and the ideal (VFT) glass transition T_0, (v) is the MCT at the current stage the only consistent way to describe the broad frequency range susceptibilities of glass-forming liquids, and (vi) since the MCT is based on density fluctuations, is it applicable to depolarized scattering in optically anisotropic materials, where first-order scattering from orientational fluctuations may be dominating at low frequencies?

Some of these problems are currently under study in our laboratory.

ACKNOWLEDGMENTS

Partial financial support of the Sonderforschungsbereich 262 of the DFG is gratefully acknowledged. The authors would like to thank Professor H. Z. Cummins and Dr. M. Fuchs for extensive discussions.

[1] W. Steffen, A. Patkowski, G. Meier, and E. W. Fischer, J. Chem. Phys. **96**, 4171 (1992).
[2] G. P. Johari and M. Goldstein, J. Chem. Phys. **53**, 2372 (1970).
[3] F. Fujara, B. Geil, H. Sillescu, and G. Fleischer, Z. Phys. B **88**, 195 (1992).
[4] W. Petry, E. Bartsch, F. Fujara, M. Kiebel, H. Sillescu, and B. Farago, Z. Phys. B **83**, 175 (1991).
[5] M. Kiebel, E. Bartsch, O. Debus, F. Fujara, W. Petry, and H. Sillescu, Phys. Rev. B **45**, 10 301 (1992).
[6] F. Fujara and W. Petry, in *Polymer Motion in Dense Systems,* edited by D. Richter and T. Springer, Springer Proceedings in Physics Vol. 29 (Springer-Verlag, Berlin, 1988), p. 149.
[7] G. Meier, B. Gerharz, D. Boese, and E. W. Fischer, J. Chem. Phys. **94**, 3050 (1991).
[8] W. Götze, in *Liquids, Freezing and the Glass Transition,* Les Houches Summer School, Session LI, edited by D. Levesque, J. P. Hansen, and J. Zinn-Justin (Elsevier, Amsterdam, 1991).
[9] W. Götze and L. Sjögren, Rep. Prog. Phys. **55**, 241 (1992), and references cited there.
[10] G. Li, W. M. Du, A. Sakai, and H. Z. Cummins, Phys. Rev. A **46**, 3343 (1992).
[11] G. Li, W. M. Du, X. K. Chen, and H. Z. Cummins, Phys. Rev. A **45**, 3867 (1992).
[12] H. Z. Cummins, W. M. Du, M. Fuchs, W. Götze, S. Hildebrand, A. Latz, G. Li, and N. J. Tao, Phys. Rev. E **47**, 4223 (1993).
[13] W. Götze, J. Phys. Condens. Matter **2**, 8485 (1990).
[14] R. J. Greet and D. Turnbull, J. Chem. Phys. **46**, 1243 (1967).
[15] E. W. Fischer, G. Meier, T. Rabenau, A. Patkowski, W. Steffen, and W. Thönnes, J. Non-Cryst. Solids **131-133**, 134 (1991).
[16] S. W. Provencher, Comput. Phys. Commun. **27**, 213 (1982); **27**, 229 (1982).
[17] W. Steffen, A. Patkowski, G. Meier, and E. W. Fischer, J. Non-Cryst. Solids (to be published).
[18] I. A. Campbell, J. M. Flesselles, R. Jullien, and R. Botet, Phys. Rev. B **37**, 3825 (1988).
[19] A. Patkowski, W. Steffen, G. Meier, and E. W. Fischer, J. Non-Cryst. Solids (to be published).
[20] G. Wahnström and L. J. Lewis, Physica A **201**, 150 (1993); L. J. Lewis and G. Wahnström (unpublished).